IDV and its Proxies

Leif Svalgaard
October 2013

Moos [1910] noted that: "perhaps the sum of all ordinates of the inequality without regard to signs which gives the average ordinate in 24 hours, may be considered as a more appropriate factor representing the variation due to disturbing effects". Now, did he mean the ordinates of the daily inequalities or of the monthly [or yearly] inequality? Bartels' [1932] interpretation was: "*s* is derived from the mean diurnal variation of H at Bombay for each single month, expressed in departures from the average, and is the sum of these departures, summed without regard to sign". Continuing with Moos describing his effort of making a list of days classified as quiet or disturbed (page 421): "[for] a list of the kind … involving a large personal equation, some additional data are clearly essential in order to make the classification more mathematically definite. The daily range, or preferably the summed ranges, figures of the diurnal inequality of each day would probably serve as the most appropriate data for this purpose..." Here we shall build on that intuition [based on Moos' extensive knowledge of the phenomenon].

To make things explicit, Figure 1 illustrates our interpretation of Moos' prescription:

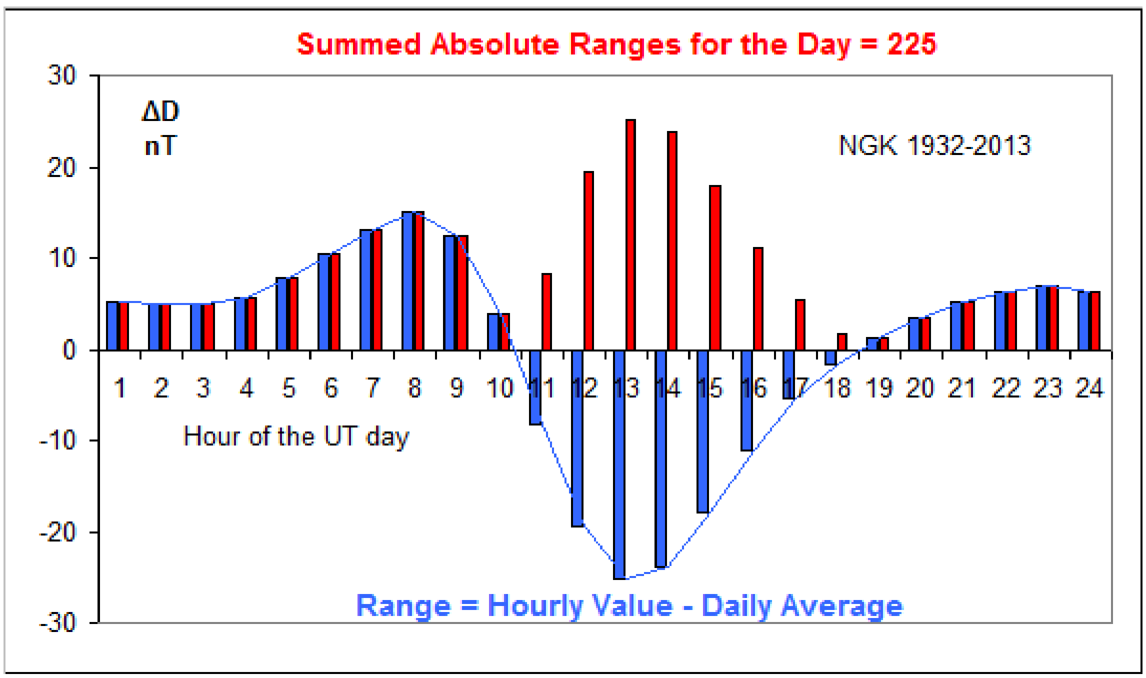

Figure 1: Average diurnal variation of Declination (expressed in force units, nT) at Niemegk. On any given day, the variation consists of a pattern as shown here [although varying a bit from day to day] with superposed 'noise' from geomagnetic activity, thus increasing the variance; this increase is what we are interested in. The signed deviations [blue bars determined every hour – either from an instantaneous value on the hour or from the hourly mean] from the daily mean are converted to unsigned departures [red bars] which are then summed over the day giving [as Moos expressed it] the Summed Ranges for each day, denoted by *s*.

We calculate *s* for both Declination, *s(D)*, and for the Horizontal Force *s(H)* initially for the German station Potsdam (POT, 1890-1907) and its replacement stations Seddin (SED, 1908-1931) and Niemegk (NGK, 1932-2012), Figure 2. Geomagnetic conditions were essentially the same at all three stations, because they were carefully placed with that in mind, so we can treat them as a single station.

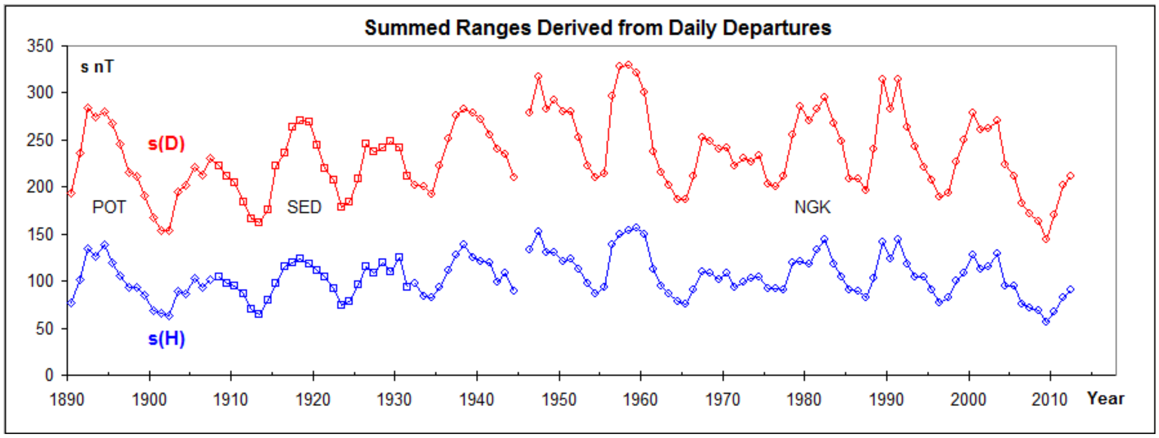

Figure 2: Summed Ranges derived from daily departures for Declination *s(D)* [red curve] and Horizontal Force *s(H)* [blue curve] for the combined POT-SED-NGK series. Each station's yearly value is marked with a different symbol [POT diamond, SED square, NGK circle]. The break in 1945 was caused by interruptions stemming from the Battle for Berlin during the final phase of WWII.

By inspection it is clear that the two series are strongly correlated. Formal analysis bears that out, Figure 3. The coefficient of determination [here and in plots to come] is calculated from the linear correlation coefficient between logarithms of the data as we are fitting a power law.

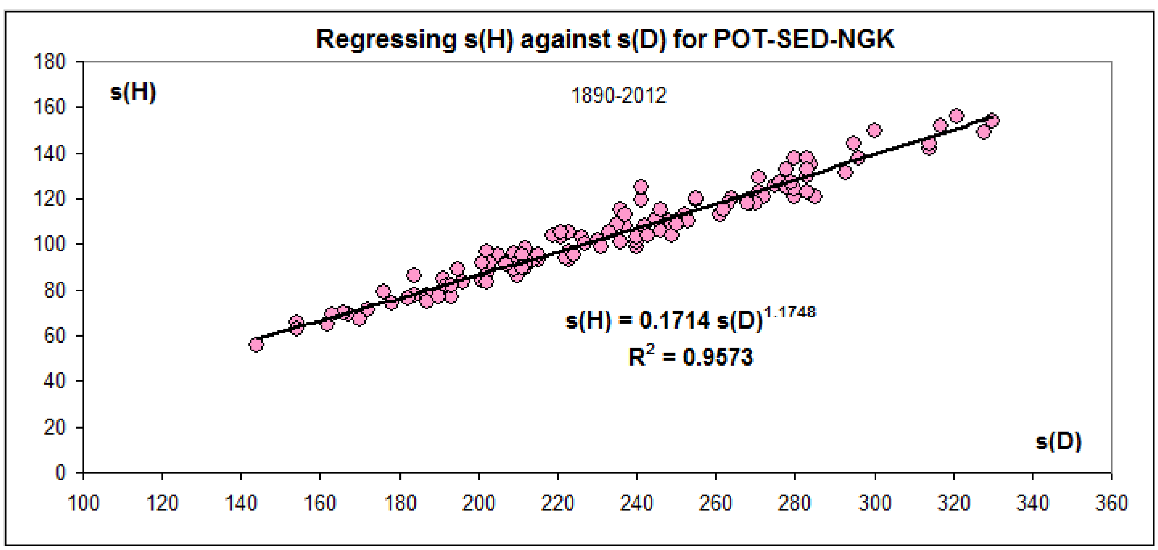

Figure 3: The average *s(H)* for each year is plotted against the average *s(D)* for that year. The data can be fitted to a power law as shown which 'explains' 96% of the correlation. We use power laws because later Figures show somewhat curved point clouds ['rivers' is probably a more descriptive term].

Using the result from the regression we can scale *s(D)* to *s(H)* and then average the scaled and the observed *s(H)*s to obtain a composite *s(H,D)* normalized to *s(H)*, Figure 4:

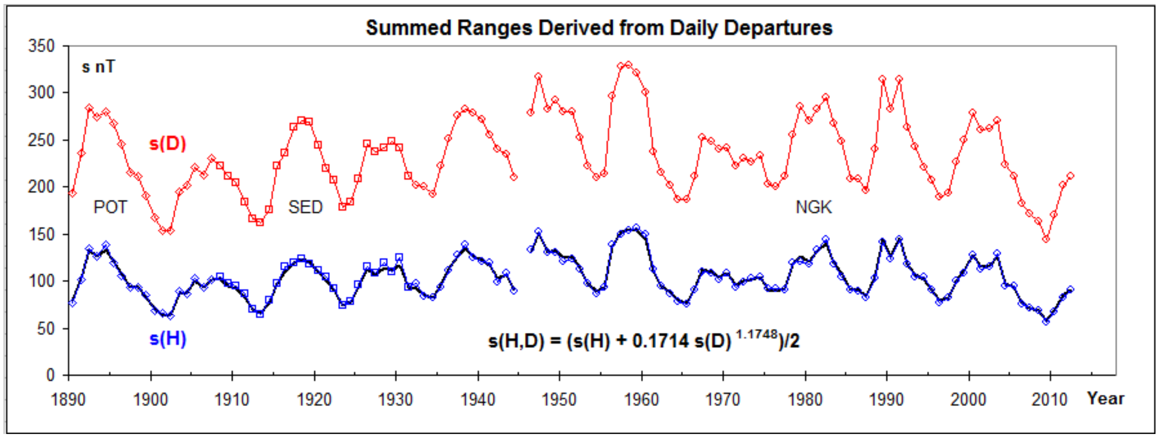

Figure 4: Summed Ranges derived from daily departures for Declination *s(D)* [red curve] and Horizontal Force *s(H)* [blue curve] for the combined POT-SED-NGK series as in Figure 2, but with the composite *s(H,D)* added over *s(H)* as a black line. It is difficult to distinguish between the blue and the black lines. It is rare in this business to find such close agreement.

We illustrate the processing steps so far with the following diagram:

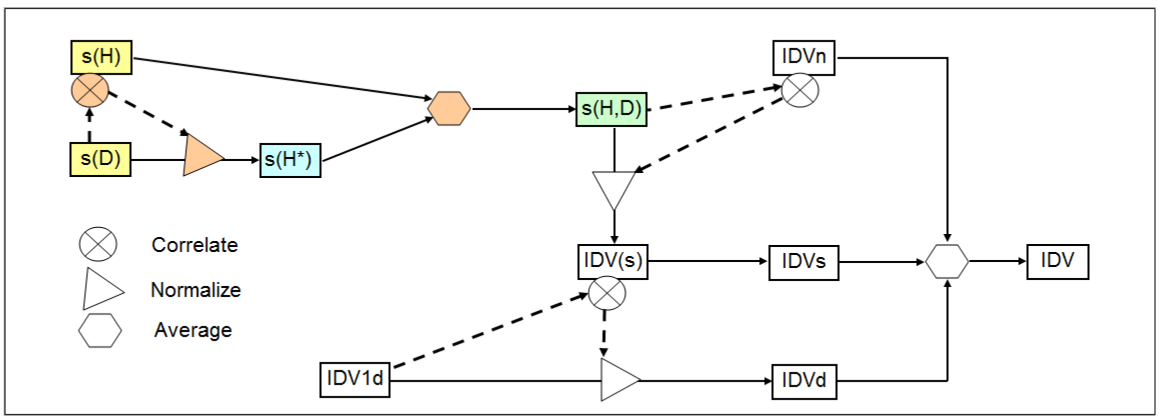

Figure 5: The observed [yellow boxes] series of Summed Ranges over a day *s(H)* and *s(D)* are correlated [orange circle with cross]. The fit is used to normalize [orange triangle] *s(D)* to the scale of *s(H)* [light blue box] which when averaged with *s(H)* [orange hexagon] yields the composite series *s(H,D)* [light green box].

Even just a cursory look at Figure 4 suggests a close correlation with the InterDiurnal Variation index, *IDV*. The *IDV* index for a given station is calculated as the average [usually over a year] unsigned differences between the hourly value [mean or instantaneous on the hour] for the hour following local solar midnight of the horizontal component of the geomagnetic field. We shall denote that quantity by *IDVn* ['n' for 'night'] in what follows. We emphasize that *IDVn* for a given station is ***local*** to the station, depending on corrected geomagnetic latitude and local underground conductivity and, in some cases, distance from the sea. We normalize *s(D)* to *s(H)* because *IDVn* is calculated for the horizontal force, *H*. Figure 6 shows the correlation [and power law and linear fits] between *s(H,D)* and *IDVn*.

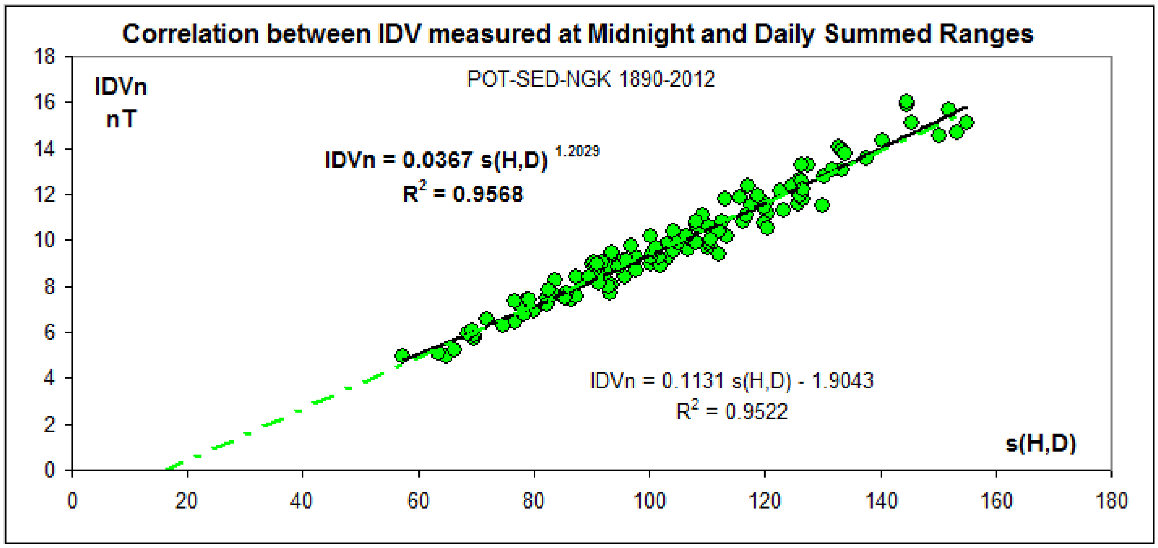

Figure 6: Correlation between yearly values of *IDVn* [midnight] and the Average Summed Ranges for the day for *H* and *D*, *s(H,D)* for the POT-SED-NGK composite series 1890-2012. The dashed line is the linear relation extrapolated to vanishing *IDVn*.

Figure 7 shows the time variation of *IDVn* and *IDV* calculated from *s(H,D)* using the power-law relation of Figure 6:

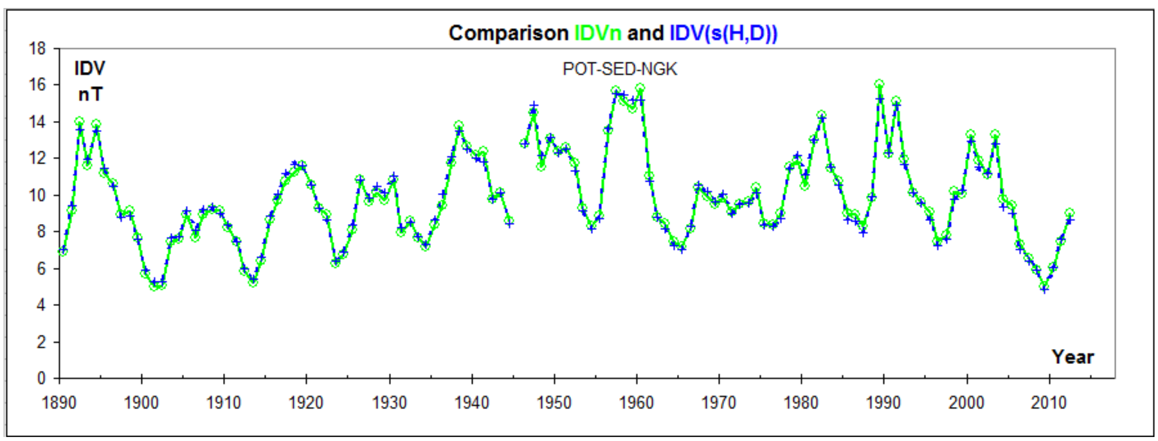

Figure 7: *IDVn* for POT-SED-NGK [green line] compared to *IDV* computed from *s(H,D)* [blue dashed line]. Because the two curves are so close to at times be indistinguishable, each yearly value is also marked with a symbol: green circle for *IDVn* and blue plus sign for *IDV(s(H,D))*. From now on, we shall use the simpler designation *IDV(s)* for *IDV(s(H,D))*.

The RMS difference between *IDVn* and *IDV(s)* is 0.27 nT out of an average value of *IDV* of 9.9 nT, i.e. less than 3%. The coefficient of determination (R^2) going from the average of *IDVn* and *IDV(s)* to *IDV09* [Svalgaard & Cliver 2010], is a remarkably high 0.9704.

As before, we illustrate the (now additional) processing steps with the following diagram:

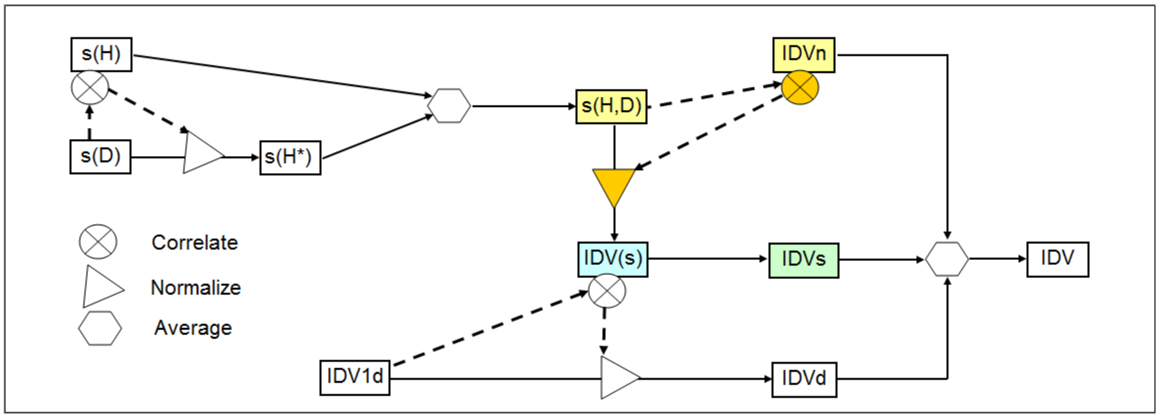

Figure 8: The observed [yellow box] series of the average Summed Ranges over a day determined from *H* and *D* are correlated [orange circle with cross] with *IDVn* [other yellow box]. The fit is used to normalize [orange triangle] *s(H,D)* to the scale of *IDVn* [light blue box] to give us an alternative series *IDVs* [light green box].

As we have already shown a decade ago [AGU Fall Meeting 2003 Poster SH21B-0108; Svalgaard & Cliver 2010: 2009JA015069] *IDV* can with good results be computed for any hour, *h*, of the day, *IDV(h)*, with due allowance for the extra variability cause by the (irregular) regular diurnal variation. Figure 9 shows the variation over time of the 24 hourly series of *IDV(h)* [the hour *h* varying from 0 to 23]. Blue [cold] colors are used for nighttime hours changing through green to red [warm] colors for the daytime:

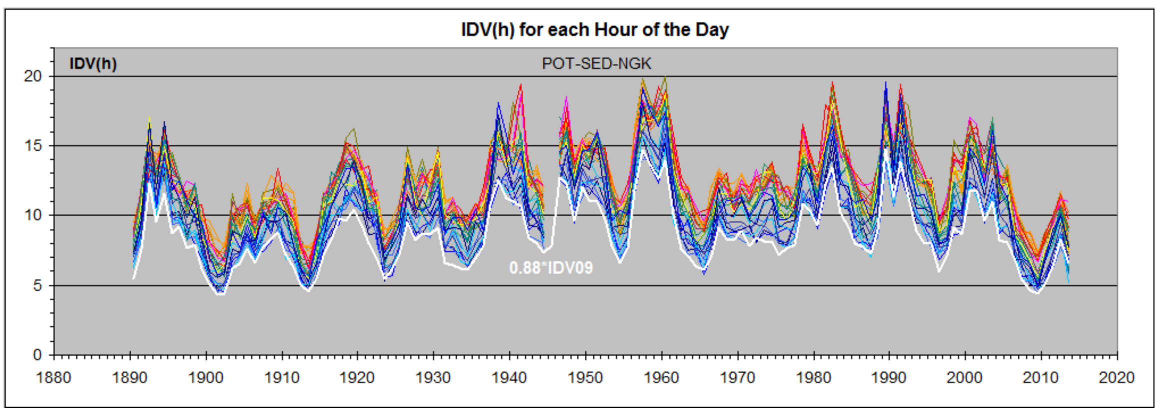

Figure 9: Yearly averages of *IDV(h)* for each hour *h* from 0 to 23 (local time) for POT-SED-NGK. Blue [cold] colors are used for nighttime hours changing through green to red [warm] colors for the daytime. Nighttime values asymptotically approach *IDV09* scaled down by a factor 0.88.

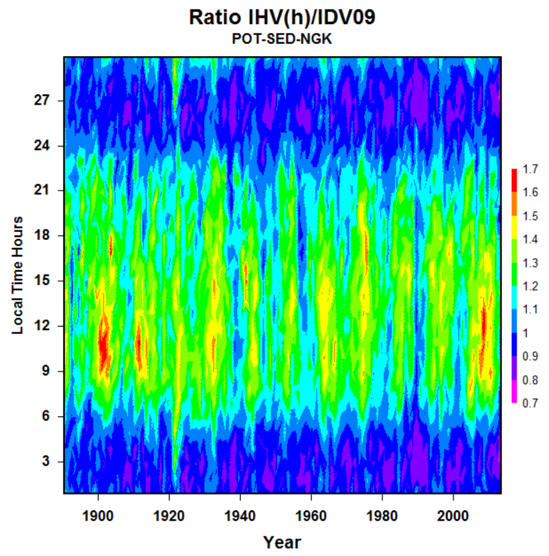

Figure 10: xxx

Xxxxxxxxxx xxxxxxxxxxxxxxxxxxx xxxxxxxxxxxxxxxxxx xxxxxxxxxxxxxxx

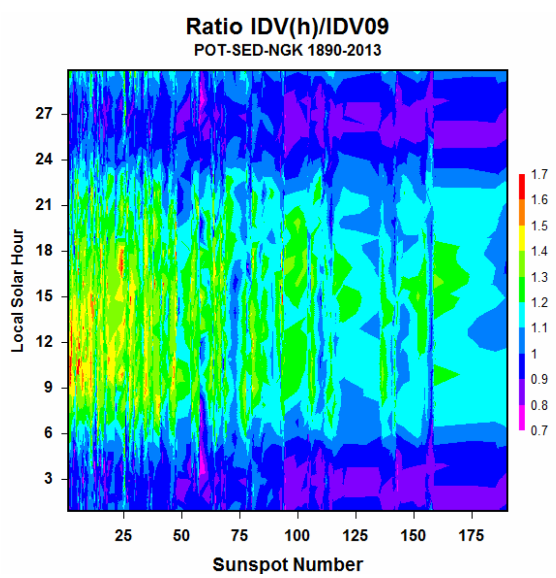

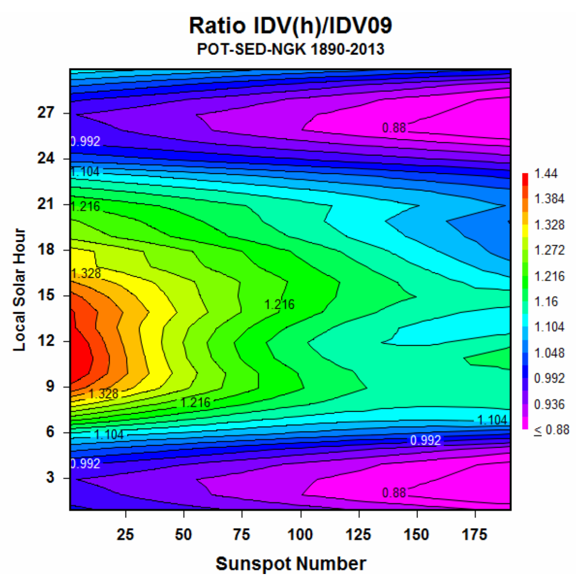

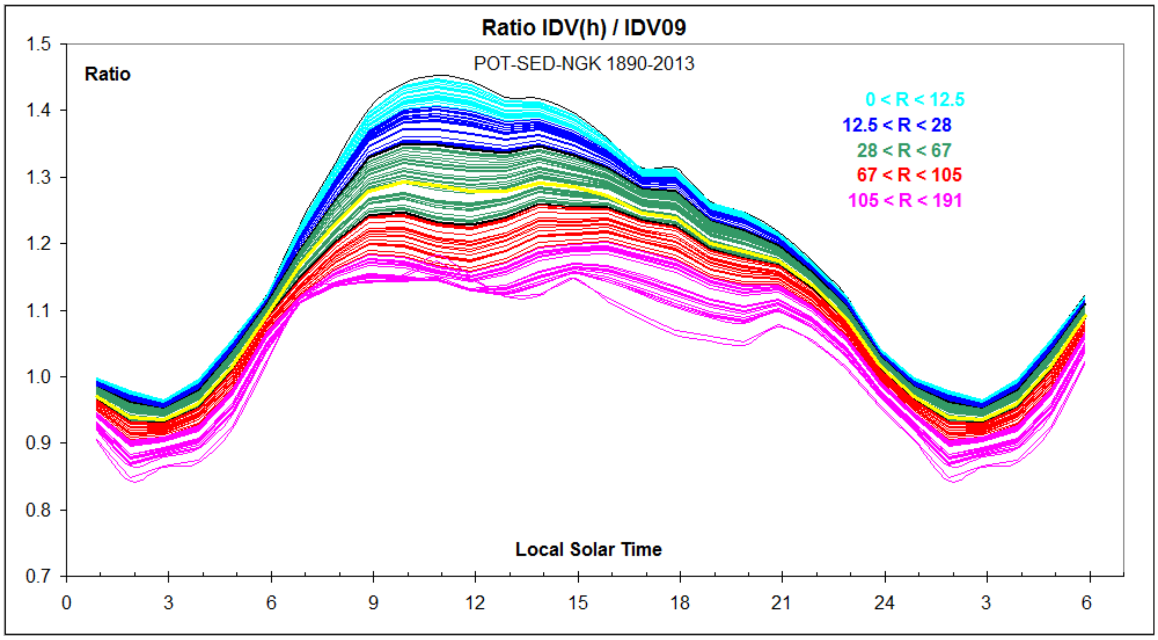
Ratio IDV(h) / IDV09
POT-SED-NGK 1890-2013
Ratio
0 < R < 12.5
12.5 < R < 28
28 < R < 67
67 < R < 105
105 < R < 191
Local Solar Time
1.5
1.4
1.3
1.2
1.1
1.0
0.9
0.8
0.7
0
3
6
9
12
15
18
21
24
3
6